A Semi-Automated Method for Measuring Fels Indicators for Skeletal Maturity Assessment in Children

Sara Gharabaghi, Thomas Wischgoll; Wright State University; Dayton, OH

Abstract

The Fels method is a well-known method for assessing the skeletal maturity from hand-wrist X-ray images. This method estimates the skeletal maturity age by manually grading multiple indicators for different hand-wrist bones. Due to the large number of indicators that need to be measured, this is a time-consuming task, especially with large databases of X-ray images. Furthermore, it can be a very subjective task that depends on the observer. Therefore, the need for automation of this process is in high demand. In this study, we have proposed a semi-automatic method to grade a sub-set of Fels indicators. This method is composed of four main steps of pre-processing, ROI extraction, segmentation, and Fels indicator grading. The most challenging step of the algorithm is to segment different bones in the Fels regions of interest (wrist, Finger I, III and V ROIs) which have been done using local Otsu thresholding and active contour filtering. The result of segmentation is evaluated visually on a subset of Fels study data set.

Introduction

In pediatric patients, skeletal maturity or bone age is an important tool for detection of hormonal, growth, or genetic disorders. Different methods, such as GP [1] and TW2 [2] methods, have been developed to assess the bone age from hand X-ray images. In GP, bone age is assessed by comparing the X-ray image with a set of reference normal images. On the other hand, in TW2, the maturity level of each bone is scored and then the overall score is calculated which corresponds to the bone age. Although GP is used more frequently because of its simplicity, the reliability of TW2 is slightly better than GP [3].

The Fels method [3] is one of the gold-standards for visual assessment methods that is reported as being more accurate than the above mentioned methods in the population of children from the United States. Furthermore, this method is the only one that provides the confidence limits of each assessment. In this approach, the skeletal age (and its confidence limit) is estimated by grading a subset of 98 skeletal indicators in the left hand-wrist radiographic (X-ray) images. At Wright State University, a longitudinal study based on the Fels method is currently performed with the first data sets dating back around 100 years resulting in an enormous data set that has to be analyzed.

Figure 1 illustrates the diagram for the wrist bones of the left hand. The Fels indicators are extracted from the Metacarpals (MET), Distal Phalanges (DP), and Proximal Phalanges (PP) of finger I, III and V, i.e. the thumb, middle finger, and ring finger. Also, Middle Phalanges (MP) indicators are measured for finger III and V. No indicators are assessed for finger II and IV because of redundancy. In the wrist region, different indicators are calculated for Radius (R) and Ulna (U) bones. These are the long bones in the wrist and every long bone is composed of two main parts: the diaphysis and the epiphysis [4]. Diaphysis is the main cylindrical shaft of a bone, whereas epiphysis represents the tips of the bone which are separated from diaphysis at the beginning of the growth process and then later ossifies over time forming the metaphysis that eventually fuses the diaphysis and epiphysis [3].

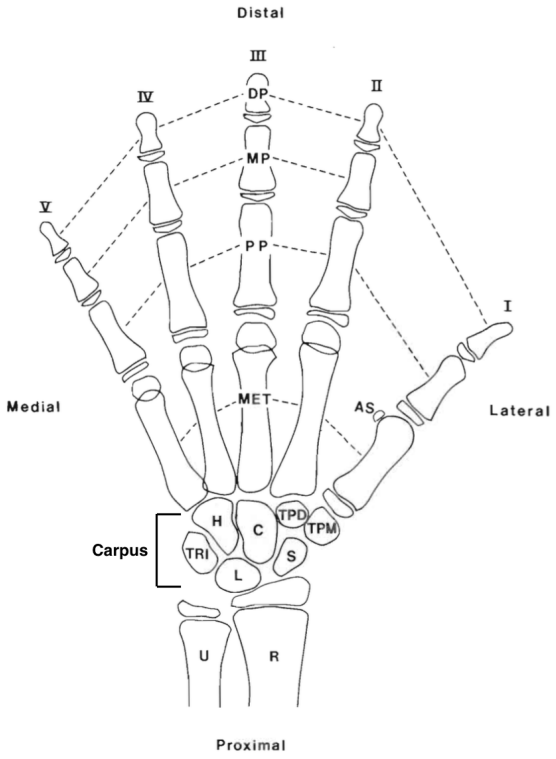

Figure 1. *Left hand-wrist bones diagram from [3]*

Generally, Fels indicators can be classified into three main groups of (1) the status of ossification, (2) the ratio of bone widths, and (3) diaphyseal-epiphyseal fusion.

Since the assessment of the Fels indicators are performed visually, the precision of this method is highly subjective and depends on the observer. Furthermore, visual assessment of a large number of images and indicators requires extra time and effort and may affect the accuracy of the results due to, for example, fatigue. Therefore, there is a high demand for making this process semi-automatic or even automatic where possible.

The objective of this study was to develop a semi-automated computer program for the assessment of skeletal maturity using the Fels indicators [6]. Our proposed method is composed of four

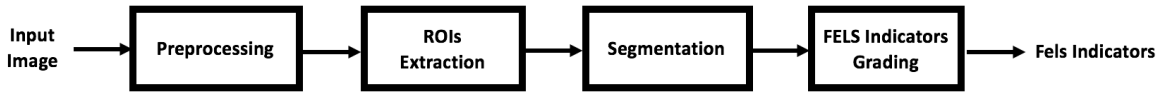

Figure 2. *Block diagram of the semi-automated bone age assessment*

main steps of pre-processing, ROIs extraction, segmentation, and Fels indicator grading which will be explained in the next section.

Segmentation is the most challenging part of this study or any other study that attempts to assess the skeletal maturity from X-ray images using any of the aforementioned methods. Several methods have been used in the literature to segment different hand bones. Some references within the literature used dynamic thresholding [7] and edge and model-based [8] approaches to segment the carpal bones. Anam et al. segmented the bones in the fingers using a knowledge-based texture analysis (fractal dimension) [9], whereas Sotocaa et al. deployed statistical point distribution and active shape models [10]. Han et al. used watershed transform and an active contour model to perform the segmentation [11]. In the proposed approach, a combination of local thresholding and active contour model segmentation methods was used to extract the bones in the wrist, finger I, III and V regions. The carpal bones have not been assessed in this study. The proposed segmentation method is evaluated visually on a subset of Fels study data set that includes hand-wrist X-ray images.

The proposed method was preliminary evaluated in two steps which have been discussed in the Results section. First, the segmentation results are evaluated visually and then, the graded indicators are compared to the ones graded manually by an expert on a set of representative images.

Methods

The proposed algorithm, which is illustrated in Figure 2, is composed of four main steps of pre-processing, ROI extraction, segmentation, and Fels indicators grading. In the following subsections, these steps are explained in detail.

The input to the proposed method is the hand-wrist X-ray image, and the output is a subset of graded Fels indicators. These indicators can be integrated to assess the skeletal age of the patient.

Pre-processing

The automatic bone age assessment is a challenging task because of poor contrast, noisy background, and hand position variation. These factors can effect the accuracy of the segmentation and bone age assessment negatively. Therefore, a pre-processing step is needed to tackle these problems before further processing. In this study, we have used a three-step pre-processing scheme that is shown in Figure 3.

First, we have analyzed the histogram of the image to decide whether the image has poor contrast. Then, the CLAHE (Contrast Limited Adaptive Histogram Equalization) [12] method is used to enhance the contrast of the image. Figure 4a and Figure 4b show the input image with poor contrast and the enhanced image, respectively.

Second, the noisy background is removed in two steps. A global threshold based on the mean intensity of the image is ap-

Figure 3. *Block diagram of the pre-processing step of the proposed method.*

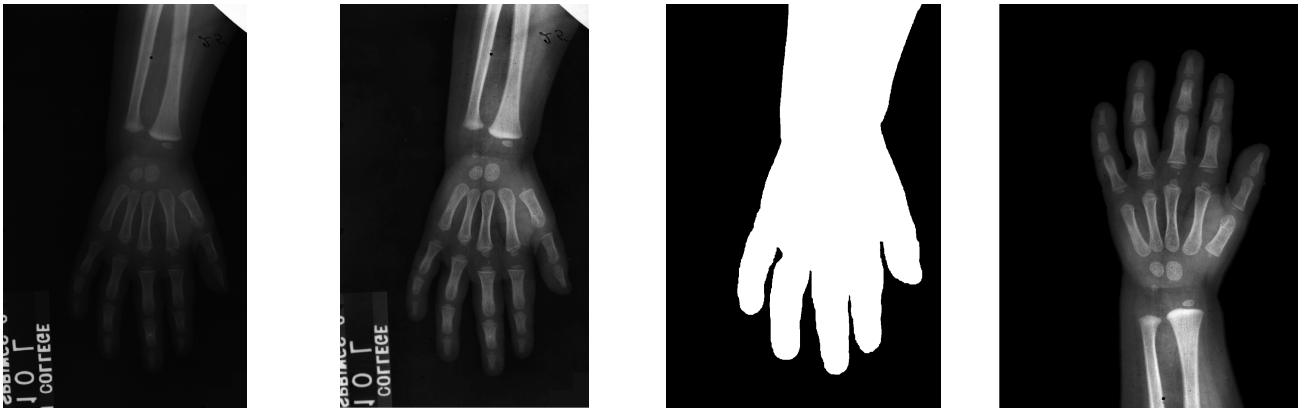

(a) Input image (b) Contrast enhanced image (c) Extracted hand silhouette (d) Output of pre-processinge step

Figure 4. *Pre-processing step of the proposed method.*

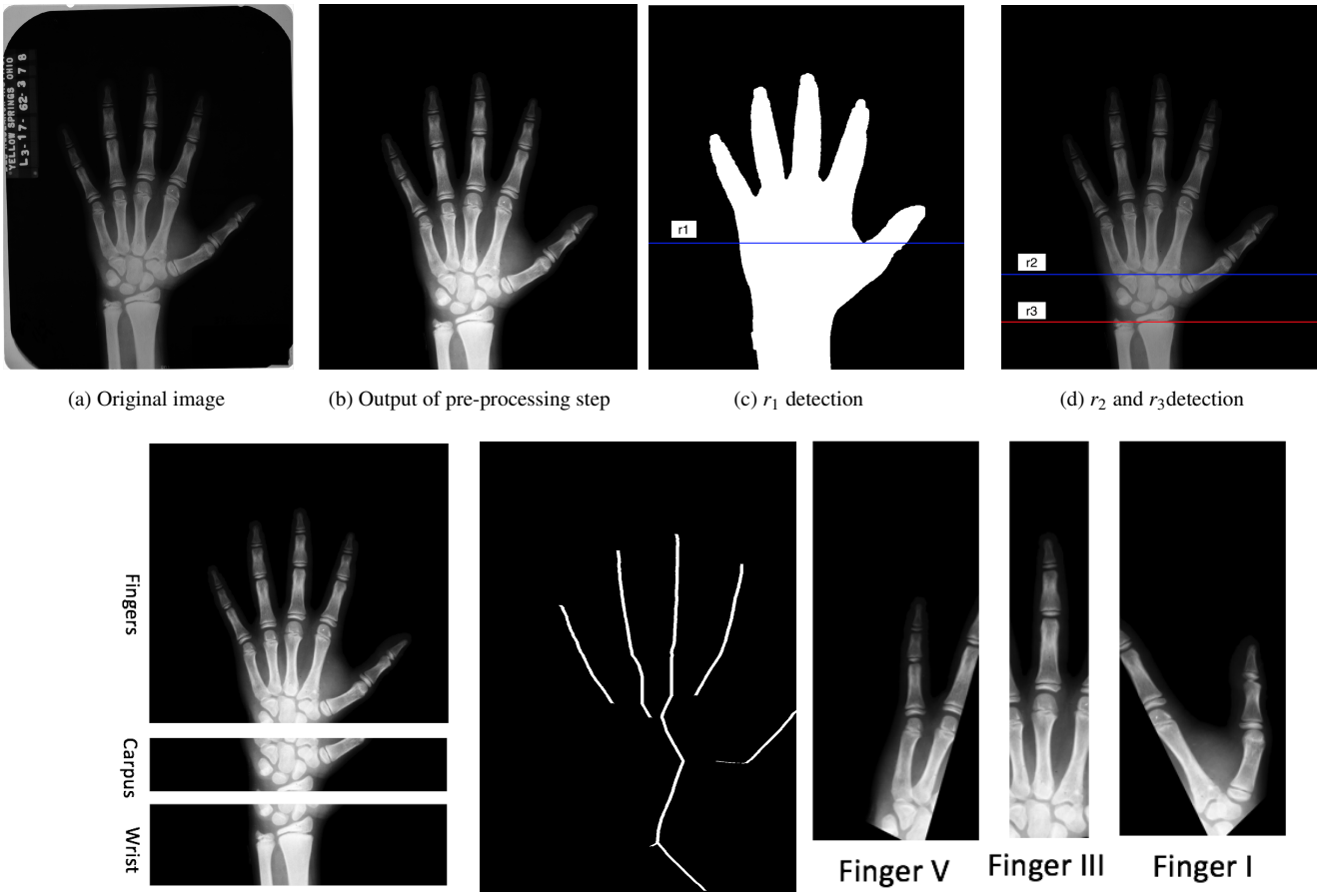

(a) Original image (b) Output of pre-processing step (c) r_1 detection (d) r_2 and $r_3$detection

(e) Extracted fingers, carpus and wrist ROIs (f) Thinned image (g) Extracted finger I, III, and V ROIs from Fingers ROI

Figure 5. *ROI extraction step of the proposed method.*

plied to the image. Then, a set of mathematical morphological filters are administered to the image in order to remove the background noise and anything around the hand by selecting the largest region in the image. This yields the extracted hand silhouette as the output. Figure 4c shows the extracted hand silhouette.

Finally, if the image is not in the standard left hand X-ray protocol view, it is reoriented, i.e. rotated, before further processing. This has been done by fitting a center-line to the extracted hand object using the least square fitting method. Then, the image is rotated to align the center-line with the vertical axis.

Figure 4d and 5b show the outputs of the pre-processing steps for the inputs shown in Figure 4a and 5a, respectively.

Region of Interests (ROIs) Extraction

The next step of the proposed method is to extract Fels ROIs from the pre-processed image. These regions of interests (ROIs) narrow down the area in which image processing algorithms have to operate to determine the grade for each Fels indicator. Specifically, the ROIs for the Fels method are the carpus, wrist, fingers I, III, and V. The method used for this purpose takes advantage of the prior knowledge on the standard hand protocol, i.e. the fact that the hand at this point is in a known orientation and location.

To determine the Fels ROI, the extracted hand silhouette is scanned row by row from the proximal end to the distal end until the last row r_1 with two zero crossing is detected (see Figure 5c). Based on our experiments, this is usually located at the middle of the metacarpals.

Then, the sum of the intensities in every row from r_1 toward the proximal end is calculated on the output of the pre-processing step. The rows r_2 and r_3 with the maximum and minimum sum of the intensities are detected (see Figure 5d). These rows are usually located at the proximal end of metacarpals and distal end of Radius, based on our experiments. The region that is limited by r_2 and r_3 is selected as carpus ROI. The row between r_2 and r_3 defines the upper edge for wrist ROI, and lower edge for fingers ROI. Figure 5e shows these ROIs.

Next, the ROIs for finger I, II and V are extracted from the previously extracted fingers ROI. This has been done by finding the finger tips using morphological thinning operators (Figure 5f)followed by the following steps to extract finger I, III and V.

Finger I ROI

For finger I, he fingers ROI is rotated to align the center-line of the finger with the vertical axis. The center-line of the rotated image will be used as the left-side edge for finger I ROI.

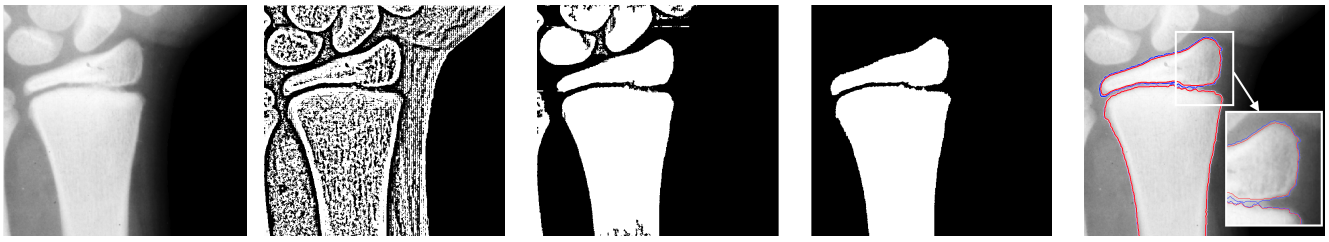

(a) Radius ROI (b) Local thresholding (c) Morphological operations (d) Using prior knowledge (e) Active countour (in red color)

Figure 6. *Segmenting radius bone from its ROI.*

(a) Wrist ROI (b) Wrist-Ulna ROI (c) Segmented Ulna (d) Wrist-Radius ROI (e) Segmented Radius - Diaphysis (f) Segmented Radius - Epiphysis

Figure 7. *Segmentation process of the proposed method.*

Finger V ROI

The fingers ROI is rotated to align the center-line of finger IV with the vertical axis. Then, the the center-line of finger IV is used as the right-side edge of finger V ROI.

Finger III ROI

In this case, the fingers ROI is rotated to align the center-line of finger III with the vertical axis. Then, maximum width of the hand silhouette is detected. This is usually wider than the sum of the width of all five fingers. Hence, this can be used as a rough estimate of the width of each finger, w_{fing}. The right and left edges of the finger III ROI are selected at the $\frac{w_{fing}}{2}$ distance from finger III center-line.

After extracting finger I, III, and V ROIs, these are rotated so that the center-line of the corresponding finger is aligned with the vertical axis. Figure 5g shows the the extracted finger I, III and V for the sample input.

As was mentioned before, the Fels indicators for the carpus region were not measured yet in this study. Hence, the current approach only utilizes the wrist and fingers I, III, and V ROIs.

Segmentation

In this step, the corresponding bones in each ROI are segmented. Figure 6 shows the segmentation process for a sample radius ROI.

The following segmentation process has been applied to each extracted ROI as determined in the previous step: First, the Otsu thresholding [13] segmentation method is applied locally to the ROI (Figure 6b). Then, a set of morphological operations are utilized to fill the bone objects and remove the soft tissues around the bones (Figure 6c). After that, prior knowledge of the expected bones in the corresponding ROIs and their location is used to detect those bones and remove any other bones within the ROI ((Figure 6d). An active contour segmentation [5] is used to smooth the edges of the segmented bones. Figure 6e illustrates the smoothed boundaries in red color comparing to the boundaries from previous step in blue color.

The prior knowledge used in this step for each ROI is as follows:

Wrist ROI

In this region, there are two main bones that need to be segmented: radius and ulna. In the left wrist-hand protocol, radius and ulna are located on the right and left side of the wrist ROI.

Based on Roche *et al.* [3], the epiphysis of radius and ulna begins to ossify usually when a child reaches 1 year of age. Therefore, in younger children, there is usually no visible epiphysis. Then, the epiphysis appears as a round object and starts to increase in size as the child grows. Eventually, the epiphysis fuses with the diaphysis. Therefore, in the wrist ROI, two long bones and possibly two separate round/oval shaped objects just above the long bones are expected.

Figure 7 shows results of the the segmentation process for a sample wrist ROI shown in Figure 7a. Figure 7b and 7d shows the radius and ulna ROIs. The segmented ulna is shown in Figure 7c. Examples of a segmented diaphysis and epiphysis of the radius bone are shown in Figure 7e and 7f.

Finger I ROI

The finger I ROI is composed of three main bones (from the proximal end toward the distal end): metacarpal I (MET-I), proximal phalanges I (PP-I), and distal phalanges I (DP-I). The epi-

(a) Finger I ROI (b) Segmented bones

Figure 8. *Segmenting bones in the Finger I ROI.*

physis of MET-I forms at the proximal end of its diaphysis and eventually fuses with it. The same pattern occurs with PP-I and DP-I. Therefore, in this region, it is expected to find three cylindrical bones (diaphyses), and possibly additional one to three round or oval-shaped bones (epiphyses).

Figure 8a and 8b show an example of the Finger I ROI and segmented bones (DP-I, PP-I and MET-I), respectively.

Finger III ROI

The finger III ROI, on the other hand, is composed of four main bones (from the proximal end toward the distal end): metacarpal III (MET-III), proximal phalanges III (PP-III), middle phalanges III (MP-III), and distal phalanges III (DP-III). The epiphysis of the metacarpal in finger III begins to form at the distal end of its diaphysis and eventually fuses with it. On the other hand, the epiphysis of the MP-II forms at the proximal end of its diaphysis and fuses with it eventually. PP-III and DP-II bones are similar to MP-II. Hence, in the finger III ROI, it is to be expected that four cylindrical bones (diaphyses) and possibly additional one to four round, oval, or wedge-shaped (epiphyses) can be detected.

Figure 9a and 9b show a sample Finger III ROI and segmented bones (DP-III, MP-III, PP-III and MET-III), respectively.

(a) Finger III ROI (b) Segmented bones

Figure 9. *Segmenting bones in the Finger III ROI.*

(a) Finger V ROI (b) Segmented bones

Figure 10. *Segmenting bones in the Finger V ROI.*

Finger V ROI

Finger V includes four main bones (from the proximal end toward the distal end): metacarpal V (MET-V), proximal phalanges (PP-V), middle phalanges V (MP-V), and distal phalanges V (DP-V). The prior knowledge for this region used within the algorithm is similar to the one described in Finger III ROI subsection.

Figure 10 shows the sample input and output of this step for a sample Finger V ROI.

Fels Indicators Grading

In this step, different indicators are graded for every bone. As it is mentioned before, these indicators can be categorized into three main groups: (1) the status of ossification, (2) the ratios of bone widths, and (3) diaphyseal-epiphyseal fusion. These groups and the way they are measured is described in the next subsections.

Group 1 Indicators

The first group of indicators is graded using the segmented epiphysis bone. If the epiphysis is absent, no object was found in the segmented image, and the indicator is graded as Grade 1 and if it is present, the indicator can be Grade 2 or 3 based on the shape of the epiphysis. These indicators are:

- R-1 indicator: for the Radius bone, if the epiphysis is circular or elliptic, the indicator is graded as Grade 2. If it is present and ovoid or its proximal margin is flattened or concave, the indicator is Grade 3. The distinction between Grade 2 and Grade 3 is decided based on the shape of the segmented epiphysis bone which is performed by calculating and comparing its diameter and analyzing the slope of the proximal edge of the bone.
- MET-I-1 indicator: If the epiphysis is present and round, the indicator is graded as Grade 2. If it is present and elliptic and its proximal margin is smooth, Grade 3 is assigned to this indicator.
- MET-V-1, PP-I-1, PP-III-1, PP-V-1, MP-III-1, MP-V-1, DP-I-1, DP-III-1, and DP-V-1 indicators: These bones are graded as Grade 2 when the center for the epiphysis of the metacarpal V is ossified.

As an example, for the Radius bone shown in Figure 11a, Grade 3 is assigned to the R-1 Indicator because the epiphysis

(a) Radius ROI (b) Radius-Diaphysis (c) Radius-Epiphysis

Figure 11. *Segmenting bones in the Radius ROI.*

(Figure 11b) is present and its proximal margin is concave.

Group 2 Indicators

The second group of indicators are the ratio of epiphysis width to the metaphysis width:

$$Ratio = \frac{Epiphyseal \quad Width}{Metaphyseal \quad Width} \tag{1}$$

The maximum width of metaphysis and epiphysis are measured at the right angle to the long axis of the bone. This indicator is not measured in case of completed fusion or absent epiphysis. So, if the algorithm could not segment the epiphysis as a separate bone, this indicator will not be graded. These indicators are R-2, U-2, MET-I-2, MET-III-2, MET-V-2, PP-I-2, PP-III-2, PP-V-2, MP-III-2, MP-V-2, DP-I-2, DP-III-2, and DP-V-2.

For measuring this group of indicators, first, the center-line of the long shaft of the bone (diaphysis) is aligned with the vertical axis. Then, the maximum metaphysis and epiphysis width are calculated for the segmented epyphysis and diaphysis of the bone. Finally, the ratio is computed.

Figure 12 shows the measured epiphysis and diaphysis width from the segmented bones on the radius ROI for calculating the R-2 indicator.

Group 3 Indicators

The third group of the indicators are related to the diaphyseal-epiphyseal fusion. Grade 1 is assigned to this group of indicators in case there is no fusion yet. If the fusion is incomplete the indicator is Grade 2, and Grade 3 once the fusion is complete. These indicators are R-8, U-3, PP-I-5, PP-III-5, PP-V-5, MP-III-5, MP-V-5, DP-I-4, DP-III-4, and DP-V-4.

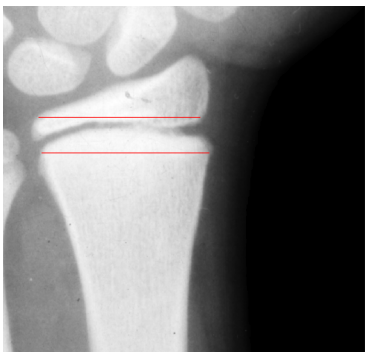

Figure 12. *Measured epiphysis and diaphysis widths for R-2 indicator.*

Note that these groups of indicators will be graded if the epiphysis of the segmented bone is present (the corresponding Group 1 indicator is not Grade 1). For these indicators, Grade 1 is assigned when the fusion is absent and epiphysis is segmented as a separate bone. In this state, a radiolucent strip is present in the whole diaphyseal-epiphyseal junction. The assignment of Grade 2 or 3 will be based on the analysis of the intensity changes between epiphysis and diaphysis. If the intensity decreases in some areas in the diaphyseal-epiphyseal junction (radiolucent strip is present partially in the diaphyseal-epiphyseal junction) then the indicator is Grade 2. In case of no radiolucent strip in the junction, Grade 3 is assigned to the indicator.

For the Radius ROI shown in Figure 11a, Grade 1 is assigned to the R-8 indicator because the ephiphysis is segmented as a separate bone and a radiolucent strip extends for the whole length of the the diaphyseal-epiphyseal junction.

Results

The proposed method that is described in the previous section is implemented in MATLAB 9.2 (Release 2017a, The MathWorks, Inc, Natick, MA, USA) and tested on a subset of the Fels study data set. The data set includes hand-wrist radiographic images of children in the range of ages 0 to 20 years. These images were stored as 16-bit digital images.

The first three steps of pre-processing, ROIs extraction, and bone segmentation are tested and evaluated visually on a subset of the available data sets including 25 X-ray images. If these steps result in the accurate segmented bones in each region, the measured indicators will be precise. This will lead to an accurate skeletal age.

In the pre-processing step of the proposed method, the hand object is extracted correctly in 21 images. In the 4 remaining images, the user is provided with an interactive GUI to set a proper threshold that results in a correct hand object boundaries. This is explained in the Discussion section.

The ROI extraction for wrist, finger I, III and V are visually evaluated to make sure that they include the bones in the corresponding region. In this step, the success rate for automatic extraction of the ROIs was 88%.

The most challenging part of this study is to segment dif-

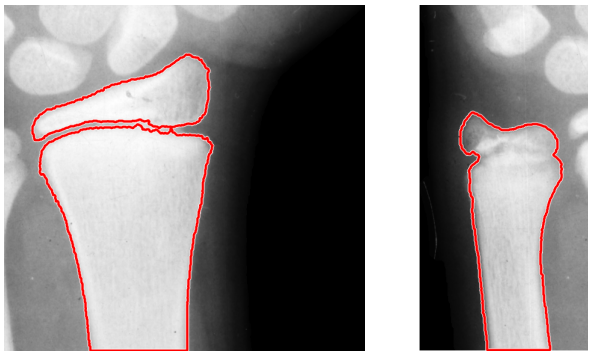

(a) Radius (b) Ulna

Figure 13. *Visual evaluation of the segmentation step for radius and ulna.*

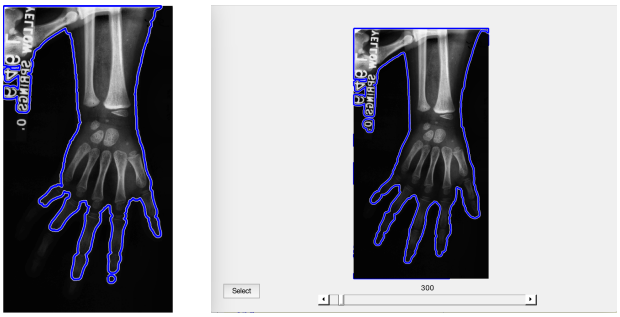

(a) (b)

Figure 14. *X-ray image with very poor contrast and the a. automatically and b. manually extracted hand silhouette boundaries.*

ferent bones accurately. If this task is performed precisely, then indicators will be graded correctly, and the resulted estimation of the skeletal maturity age will be correct. We have evaluated the segmentation step of the proposed method on images with correct extracted ROIs (22 images) by overlaying the boundaries of segmented bones on the actual image. Figure 13 shows examples of this evaluation for segmented radius and ulna using the proposed method. The success rate of this method in segmenting wrist, finger I, III, and V bones are 91%, 82%, 91% and 73%, respectively. The lower success rate of segmenting finger V bones is due to the fact that the distal and middle phalanges of finger V have very poor contrast in younger children in some images which makes the segmentation task very difficult.

The graded subset of the Fels indicators are compared with the reference values provided by well-trained specialists and examples provided in the Fels method textbook [3]. There was general agreement between the algorithmically determined grades and the ones provided by the specialists and textbook.

The time required to apply the proposed method on the input image varies between 1 to 3 minutes depending on the size of the image and the required pre-processing operations needed for that image.

Discussion

Automated skeletal age assessment is a challenging task because of the hand position variation and non-uniform background of the images as well as a significant amount of noise in some images. To overcome these challenges, we have used a pre-processing step to reduce the level of noise and enhance the contrast in the images. However, in some cases with very poor contrast or other objects around the hand, the algorithm fails to extract the correct hand silhouette (Figure 14a). For this reason, the algorithm asks the user to verify the extracted hand silhouette. If the user confirms the extracted hand silhouette the program proceeds to next step. Otherwise, the program allows the user to set a proper threshold value manually that extracts the correct hand silhouette (Figure 14b).

In this study, we have graded a subset of the Fels indicators for the bones in the wrist, finger I, III, and V regions. In future studies, additional Fels indicators can be graded to make the bone age assessment more accurate. Overall, the algorithm was successful in determining the correct grade for the majority of cases. This results in a considerable reduction of workload for the specialist to analyze and grade the Fels indicators in hundreds if not thousands of X-ray images. While it is very difficult for a computer algorithm to replace the expertise and experience of a specialist, our approach can, in addition to processing large data sets in a shorter amount of time, assist non-speicalists to obtain the skeletal age for comparison with the actual age of a patient.

Conclusion

In this study, we have proposed a semi-automated method to assess the skeletal maturity age from X-ray images by grading Fels indicators. This is a challenging task because of the poor contrast, hand position variation, and non-uniform background of the X-ray images. Therefore, our proposed method starts with a pre-processing step to overcome these challenges. Next, the ROIs including the bones of interests are extracted. Then, the expected bones in each ROI are segmented using a local thresholding and active contour segmentation methods. Finally, a subset of Fels indicators are graded for the segmented bones. The segmentation method was evaluated visually on a subset of Fels data sets to determine the accuracy of the segmentation step as well as the grading of the Fels indicators based on input from domain specialists. The algorithm was generally successful in grading these indicators accurately in the majority of cases leading to a significant workload reduction for the domain specialist.

Acknowledgments

We would like to thank Dana Duren, Richard Sherwood, and Carol Cottom for their assistance in providing the data sets and input as domain specialists to ensure the correctness of our results. In addition, we thank the Boonshoft School of Medicine at Wright State University for their support of this project.

References

[1] W. W. Greulich, S. I. Pyle. Radiograph Atlas of Skeletal Development of the Hand and Wrist. 2nd ed. Stanford, California, USA: Stanford University Press; 1959.

[2] J. M.Tanner, R. H. Whitehouse, N. Cameron,W. A. Marshall , M. J. Healy and H. Goldstein, Assessment of skeletal maturity and prediction of adult height (TW2 method). London: Academic Press;1983.

[3] A. F. Roche, W. C. Chumlea and D. Thissen, Assessing skeletal maturity of the hand-wrist: FELS method. Springfield: Charles C Thomas. Publisher, pp. 62-77 (1988).

[4] K. T. Patton and G. A. Thibodeau, Anthony's Textbook of Anatomy

and Physiology, 19 ed., Mosby (2009).

[5] V. Caselles, R. Kimmel, and G. Sapiro, Geodesic Active Contours,International Journal of Computer Vision, Vol. 22 (1), 61-79 (1997).

[6] N. Zhihong, Computer-Based Skeletal Age Assessment Using Hand/Wrist Radiographs in Children 8-18 Years Old, Electronic Thesis. Wright State University. https://etd.ohiolink.edu (2010).

[7] E. Pietka, L. Kaabi, M. L. Kuo, H. K. Huang. Feature extraction in carpal bone analysis, IEEE Transactions on Medical Imaging, Vol. 12 (1993).

[8] A. Zhang, A. Gertych, and B. J. Liu, Automatic bone age assessment for young children from newborn to 7-year-old using carpal bones, Computerized Medical Imaging and Graphics 31, 299310 (2007).

[9] S. Anam, E. Uchinom and Noriaki Suetake, Hand bones radiograph segmentation by using novel method based on morphology and fractal, SCIS and SCIS (2014).

[10] J. M. Sotocaa, J. M. Inestab and M. A. Belmonte, Hand bone segmentation in radioabsorptiometry images for computerised bone mass assessment, Computerized Medical Imaging and Graphics, 27, 459467 (2003).

[11] C. C. Han, C. H. Lee and W. L. Peng, Hand radiograph image segmentation using a coarse-to-fine strategy, Pattern Recognition, 40, 29943004 (2007).

[12] K. Zuiderveld, Contrast Limited Adaptive Histogram Equalization, Graphic Gems IV, San Diego: Academic Press Professional, 474485 (1994).

[13] N. Otsu, "A Threshold Selection Method from Gray-Level Histograms," IEEE Transactions on Systems, Man, and Cybernetics, Vol. 9, No. , pp. 62-66 (1979).

Author Biography

Sara Gharabaghi received her Bachelor's and Master's degree in biomedical engineering and electrical engineering from Sahand University of Technology, Iran in 2009 and 2011, respectively. She is currently working toward her PhD degree in computer science at Wright State University, Dayton, OH. Her research interests are biomedical image processing and analysis, retinal image registration, and super-resolution reconstruction of MRI images.

Thomas Wischgoll received his Master's degree in computer science in 1998 from the University of Kaiserslautern, Germany, and his PhD from the same institution in 2002. He was working as a post-doctoral researcher at the University of California, Irvine until 2005 and is currently an full professor and the Director of Visualization Research at Wright State University. His research interests include large-scale visualization, flow and scientific visualization, as well as biomedical imaging and visualization. In the area of vector field visualization, Dr. Wischgoll completed the topological analysis of vector fields by developing an algorithm that detects closed streamlines, a missing link between branches of a topological skeleton. In the realm of biomedical engineering, he developed a visualization system that facilitates the analyses of large-scale vascular models of a heart represented geometrically by several hundred million polygons. The models are derived from CT scans and feature a simulated flow inside the blood vessels. Dr. Wischgoll developed methodologies for analyzing such volumetric data and extracting quantitative measurements at very high accuracy for further analysis. His research work in the field of large-scale, scientific visualization and analysis resulted in more than fifty peer-reviewed publications, including IEEE and ACM. Dr. Wischgoll is a member of ACM SIGGRAPH, IEEE Visualization & Graphics Technical Committee, and the IEEE Compute Society.